

Synthesis of borate modified bioactive glass scaffold using PVP burning-out method for bone tissue replacement

Amr M. Abdelghany^{1,2*}, Mahrous S. Meikhail³, Ehab Hegazy⁴, Shalabya I. Badr³, Dina A. Agag⁵

¹Spectroscopy Department, Physics Division, National Research Center, 33 ElBehouth St., 12311, Dokki, Cairo, Egypt.

²Basic Science Department, Horus University, International Coastal Rd, New Damietta, 34518, Damietta, Egypt

³Physics Department, Faculty of Science, Mansoura University, 35516, Mansoura, Egypt

⁴Basic Science Department, Faculty of Pharmacy, Delta University, 11152, Gamasa, Egypt

⁵Basic Science Department, Faculty of Physical Therapy, Delta University, 11152, Gamasa, Egypt

*corresponding author e-mail address: a.m_abdelghany@yahoo.com

ABSTRACT

Three-dimensional (3D) bioactive glass scaffolds are one of the most studied types of scaffolds for bone tissue replacement because of their excellent bioactivity and potential for stimulating osteogenesis and angiogenesis. In the present study, modified Hench-based bioglass was fabricated by polyvinyl pyrrolidone (PVP) burning-out method for producing porous scaffold. In vitro investigation of the scaffolds' bioactivity was achieved through examining changes in its composition during exposing to physiological simulated body fluid (SBF) solution via Fourier transform-infrared (FT-IR) absorption spectroscopy, X-ray diffraction (XRD) analysis, Scanning electron microscopy (SEM) supported by Energy-dispersive X-ray (EDX). FT-IR spectral data was used to validate the formation of hydroxyapatite as an indication of the bioactivity potential of the studied scaffold post incubation in SBF. The prepared samples were examined by XRD to recognize the crystalline phase/phases that may formed after immersion in physiological solutions and supported via (SEM/EDX) data.

Keywords: Borate bioactive glass; Polyvinyl pyrrolidone (PVP); Simulated body fluid (SBF); Hydroxyapatite (HA); In vitro test; Bone Tissue Replacement.

1. INTRODUCTION

Glasses are playing a very vital role in the progress of society. Glasses are applied to numerous fields such as architecture, telecommunication, automation etc. Recently a new class of glasses is being developed to be used in biomedical applications i.e. glass ceramics and bioactive glasses [1, 2]. Nowadays, bioactive glasses are being used in dental prosthetics, orthopedics, especially for bone regeneration, or to provide a substitute for defective parts, owing to their tendency to form the direct bond with the living tissue after implanting in the human body. Recently, such materials gain a great courtesy to be applied in soft tissue repair according to their aptitude to promote angiogenesis (formation of blood vessels) [2, 3].

On the level of the human skeleton- With respect to skeletal anatomy, bone defects can result in loss of mobility and can be significantly debilitating. Tissue engineering has appeared as an auspicious methodology for the processes of bone repair and regeneration in the cases of tumor, trauma, osteoarthritis and decrease in bone density when the human body is not able to produce new bone material, resulting in bone resorption rate much higher than bone deposition rate (as in osteoporosis). In the most common approach, porous biocompatible implants are used, with a well-defined architecture that can replicate the strength, morphology, porosity, bioactivity and load-bearing ability of living bone. These implants serve as a temporary structure for cells and guide their proliferation and differentiation into regenerated bone tissue [2, 4, 5].

Hydroxyapatite is one of the more biocompatible replacement materials for skeletal applications and has the

chemical formula, $\text{Ca}_5(\text{PO}_4)_3(\text{OH})$ [6]. Prof Larry Hench conducted experiments where he developed a material using silicate glasses to interact with Ca and P in the body to assist in bone regeneration. This material resembles bone constituents and stimulates the growth and re-regeneration of new bone material. Thus, due to its biocompatibility and osteogenic capacity it came to be known as "bioactive glass or bio glass". The bioactive glass or bio glasses were generally used for bone replacement therapy. Usually these bio glasses can degrade within body fluid or blood plasma naturally present in our bodies to form bone-like tissues. The first Hench's patented bio glass (45S5) composed of: 45% silica (silicon dioxide SiO_2), 24.5% lime (calcium oxide CaO), 24.5% soda (sodium oxide Na_2O), and 6% phosphorous pentoxide (P_2O_5), all in weight percentage. Bioglass material is composed of minerals that are naturally occurring in the body (Ca, Na, O, H, and P), and the molecular proportions of the calcium and phosphorus oxides are similar to those in the bones. After the implantation of bioglass in the body or when it is subjected to an aqueous solution, or body fluids, converts to a silica- $\text{CaO}/\text{P}_2\text{O}_5$ -rich gel layer that subsequently mineralizes into hydroxycarbonate in a matter of hours. More the dissolution, better the bone tissue growth. This gel layer resembles hydroxyapatite matrix so much that osteoblasts were differentiated and new bone was deposited [7, 8, 9].

The requirement of high melting temperature (usually more than 1200°C) of the silicon based bioactive glasses [10] beside the harmful effect of silicon ions in the healthcare, human body free from silicon ions in their constitution so these ions remain in the

body for a long time after implantation [11], the researchers begun towards the subsequent introduction of B_2O_3 replacing SiO_2 in the patented bioglass and the derived glasses reveal acceptable bioactivity when immersed in simulated body fluid (SBF). Rahaman et al studied fully replacement of SiO_2 in traditional Hench bioglass with B_2O_3 . They also used K_2HPO_4 solution as an ersatz for SBF solution at normal body temperature ($37^\circ C$) and they observed formation of hydroxyapatite layer similar to that formed by the silicate based 45S5. The in vitro formation of HA from the borate based 45S5 bioglass led to further investigation in vivo [11, 12, 13]. Day et al. have examined the borate glasses in vitro experiment and have identified rapid conversion to HA and osteo-conductivity and reached the conclusion that borate glass can be considered as an attractive bone substitute [14].

The porous scaffold is a fundamental component for a tissue engineering (TE) strategy because it supplies a temporary three-dimensional (3D) porous matrix for premier cell proliferation, differentiation in addition to extracellular matrix production and supplying a model for new tissue regeneration [15]. Moreover, it stockpiles tissue growth requirements from nutrients, water, and growth factors. Both the scaffold material

2. MATERIALS AND METHODS

2.1. Glass preparation.

Bioactive glassy samples of nominal composition [$45B_2O_3$, $24.5CaO$, $24.5Na_2O$ and $6P_2O_5$ (mol. %)] were synthesized using analytical grade chemicals using ordinary melt annealing route. Starting material including boric acid (H_3BO_3) as a source of B_2O_3 supplied by Raysan Chemical Co., both sodium oxide and calcium oxide was added in their respective carbonate partner form supplied by El-Nasr Pharmaceuticals, Egypt, phosphorus pentoxide was added in the form of ammonium di-hydrogen phosphate ($NH_4H_2PO_4$). Calculated batches were mixed in agate mortar and melted at $1200^\circ C$ in a high temperature furnace (Lenton). Melted amples rotated occasionally every 30 min. to obtain homogenous bubble free samples after beading in a stainless mold. Obtained samples were then incubated in a controlled muffle furnace adjusted at $350^\circ C$, switched off and retained to cool gradually by a rate of $20^\circ C/h$ to remove residuals of thermal stresses. Synthesized glasses were crushed in a porcelain mortar and sieved to obtain homogenous fine particles.

2.2. Glass-derived scaffold.

The porous scaffold fabricated by the polyvinyl pyrrolidone (PVP) burning-out method through mixing of appropriate amount of viscous pre-dissolved PVP solution and powdered boro-phosphate glass. A homogenous blend of PVP solution and the glass base powder was obtained by stirring. The mixture was then pressed into a cylindrical stainless steel mould (diameter: 10 mm) by using an automatic hydraulic press (applied stress: 120 MPa). Subsequently, the pressed disks were drying overnight at room temperature then treated through a sintering process to consolidate their structure and to burn off the polymer additives in the glass.

2.3. In vitro bioactivity evaluation. In vitro bioactivity test was assessed by exposing the modified glass samples to the simulated

and its architectural design (pore size, porosity and interconnectivity) play a significant role in governing tissue regeneration and define the ultimate shape of newly grown soft or hard tissue [15, 16]. The ability to design novel porous scaffold with controllable and satisfactory bioactivity is of significance. Researchers are interested in the bioactivity of the glasses and use different approaches to study it.

The presented work aims to study the bioactivity of a synthesized porous bioglass based on full substitution of B_2O_3 for SiO_2 in the Hench's patented Bioglass[®] by the exposing to simulated body fluid (SBF) for prolonged time (1 week→8 weeks) at body temperature $37^\circ C$. The porous scaffold fabricated by using polymer burned-out method. FT-IR optical absorption spectral data for the studied samples before and after prolonged immersion times in the physiological SBF solution were performed to retrace glass network structural variations involved together with the conversion of the prepared samples to hydroxyapatite as an indication for bioactivity and bone bonding ability. Further study was devoted to exploring earlier investigation of the bioactivity of such glasses using simple mixed mathematical spectroscopic techniques for analysis.

body fluid (SBF) performed according to the recipe reported by Kokubo et al. [17, 18] and remembered in the numerous published articles, for example Ref. [19, 20]. SBF is an acellular aqueous medium with inorganic ion composition nearly similar to that of the human blood plasma. SBF solution was prepared by mixing the appropriate amounts of sodium chloride (NaCl), sodium hydrogen carbonate ($NaHCO_3$), potassium chloride (KCl), di-potassium hydrogen phosphate trihydrate ($K_2HPO_4 \cdot 3H_2O$) and magnesium chloride hexahydrate ($MgCl_2 \cdot 6H_2O$), calcium chloride ($CaCl_2$), sodium sulfate (Na_2SO_4) in deionized water with the help of magnetic stirrer in a beaker, according to the concentrations given in Ref. [17–20]. Then, the solution was buffered to $pH = 7.4$ with tris-hydroxymethyl-amino-methane [$(CH_2OH)_3CNH_3$] and one molar-hydrochloric acid (1M-HCl).

The in-vitro test was carried out in static regime at $36.5^\circ C$ for the following time intervals: 1 week, 2, 4, 6, and 8 weeks. The samples were placed individually in the plastic containers in a volume of model solution corresponding to $S_a/V_s \sim 10\text{ cm}^{-1}$ (Equation 1) in reference [21]. After each interval time one sample was removed, then gently rinsed with deionized water and dried in air at room temperature for further analysis. During the incubation time, the SBF solution was replaced every two days to avoid ionic depletion in the SBF due to the precipitation of inorganic salts on the disk' surface.

2.4. Structural and spectroscopic analysis of the modified boro-phosphate glass.

Fourier transform infrared (FT-IR) absorption spectra of the modified glasses were measured at room temperature ($\sim 37^\circ C$) in the wavenumber range of $4000 - 400\text{ cm}^{-1}$ using FT-IR spectrometer (type nicolete IS10, USA). Fine powder of the specimen mixed with KBr in the ratio 1:100 for quantitative

analysis and the mixture was subjected to a load of 5 t/cm² in an evocable die to make clear homogeneous discs. After that the FT-IR absorption spectra were immediately measured after preparing the discs to avoid moisture attack. The measurements were taken for the studied samples before and after exposing to SBF solution for two months.

The compositional and crystallinity of the samples were analyzed by X-ray diffraction to identify the structural changes after exposing to SBF solution. Fine powder from samples was

3. RESULTS

3.1. Fourier transforms infrared (FT-IR).

FT-IR absorption spectra acted as the finger prints of the detailed structural network forming units in the studied glasses in analogy with their corresponding crystalline analogues. The base of the studied glass formed from two main glass-forming oxides: B₂O₃ 45% and P₂O₅ 6% and with two additional modifier oxides CaO 24.5% and Na₂O 24.5%. The main units of the studied glass network former, BO₄ and BO₃ groups for the borate glass former and PO₄ groups for the phosphate former, exhibited vibrational bands in the same region of the FT-IR absorption spectra so the overall spectra curves of the studied sintered glass SG and SG-PVP before and after chemical treatment with the SBF solution reveal compact interlinked numerous vibrational bands especially concentrated within the mid wavenumber range 400 to 2000 cm⁻¹, as shown in Figure 1 and 2. The born proportion was greater than that of the phosphate in the studied glass so it was expected that the main features of the FT-IR spectra belong to the boron former units.

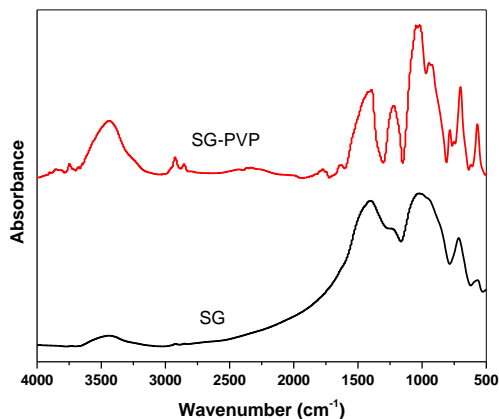


Figure 1. FT-IR spectra of the modified sintered glass SG and SG-PVP.

The FT-IR spectra of the studied glass before immersion can be divided into the following regions:

- (i) 630 - 400 cm⁻¹ is related to the bending vibrations of the O=P-O linkages. This region may be superimposed with the vibrations of modifiers ions (Na⁺, Ca⁺²).
- (ii) 810 - 630 cm⁻¹ is attributed to the bending vibration of B-O-B in BO₃ units.
- (iii) 1152 - 810 cm⁻¹ is related to the stretching vibrations of B-O groups in tetrahedral borate units in different forms overlapped with the vibrational bands of P-O, PO₂ groups.
- (iv) 2000 - 1152 cm⁻¹ is related to B - O stretching vibrations of [BO₃] units also this band ended with a small shoulder at about 1659 cm⁻¹ appeared after polymer adding to sintered glass may be attributed to C=O carboxylic stretch region the interaction

examined using PANalytical X'Pert PRO system. This system used CuK_α radiation (where, the tube operated at 30 kV, λ = 1.540 Å, the Bragg's angle (2θ) in the range of 4-70°).

Scanning electron microscopic (SEM) was performed on samples at room temperature to determine the changes on the surface morphology of the modified glass using an SEM Model Philips XL 30 attached with EDX Unit. This system operated at accelerating voltage 30 KV, with a magnification 10X up to 400.000X.

happened between polymer and modified sintered glass as shown in Figure 1.

- (v) the near region from FT-IR spectra distinguish by small peaks identified at 2847, and 2920 cm⁻¹ and a broad band centered at 3436 cm⁻¹, this region related to water and OH vibrations. The existence of OH bonds and water vibration indicate the hygroscopic nature of the modified glass.

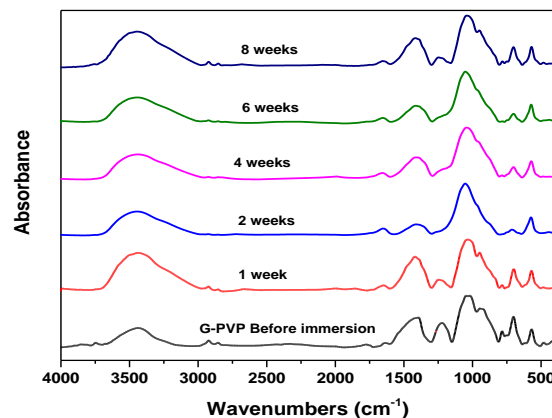
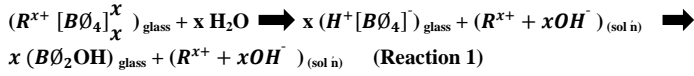


Figure 2. FT-IR spectra of the modified SG-PVP before and after exposing to SBF solution.

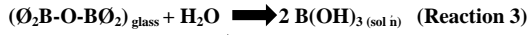
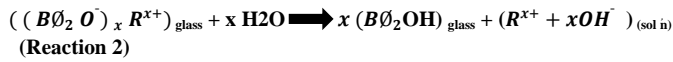
To get quantitative and detailed information about the changes that happened in the structural groups of the modified scaffold after exposing to the SBF solution, the spectra were deconvoluted into Gaussian bands. Only the 2000 - 400 cm⁻¹ range was considered for the deconvolution process and least square method was used to analyze the graphs. Figure 3 represents the deconvoluted spectra of the modified scaffold before and after exposing to SBF solution for a period extended to eight weeks. The deconvoluted spectra illustrated that the intensities of some of the absorption peaks varied after exposing to the SBF solution in comparison with their intensities before exposing. This result may be due to the differences in the solubility degree of the two main network formers involving the two main borate species with triangular and tetrahedral coordinates and the secondary phosphate species. The explaining of this result indicated by plotting the relation between the fraction concentration of four coordinates groups B₄ with the immersion time, as shown in Figure 4. The relation indicated that the corrosion reaction takes place into four stages.

When the modified scaffold exposed to SBF solution, the trigonal borate groups dissolved quickly into borate species released into the solution. This led to sharp decrease in the concentration of these groups rather than that of four coordinates (BO₄+PO₄) units, the tetrahedral borate groups are consisting of boron connected in

four equal directions with oxygen and this makes such tetrahedral groups relatively more stable and resistance to attack than the boron connected to three oxygen in trigonal species so the BO_3 groups dissolved firstly before BO_4 groups then the tetrahedral borates unites begun to dissolve and converted to trigonal borate units according to the following reaction.



This conversion produces increasing in trigonal units led to a decrease in the concentration of B_4 fraction with immersion time. After that, the dissolving of both trigonal and tetrahedral borate groups occurred simultaneously and converted to borate species released in the solution (reaction 1, 2, 3, 4). The dissolution of the modified glass and releasing the ion from its surface led Ca^{2+} ions to react with phosphate anions in solution to form a Ca-phosphate phase on the glass surface and reached to supersaturation case after two weeks.



The net effect of glass dissolution on the accumulation of the apatite layer reached to maximum saturation that obstructs the corrosion mechanism resulting in abruptly decreasing in B_4 again.

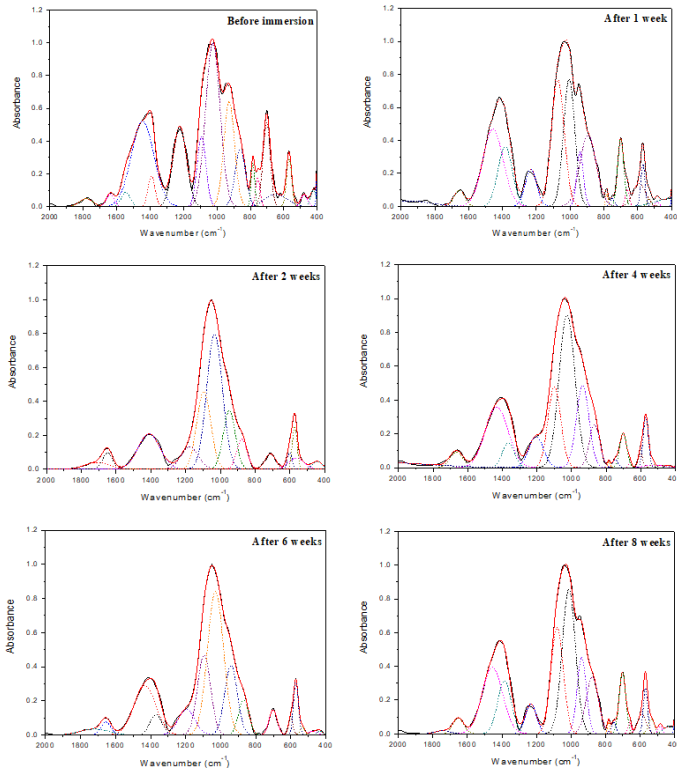


Figure 3. The deconvolution spectrum of the modified SG-PVP glass before and after exposing to SBF solution.

3.2. X-ray diffraction (XRD).

The bioactivity of modified sintered glass (SG-PVP) was assessed in vitro using SBF solution. Figure 5 illustrates the XRD pattern of modified sintered glass surface those incubated for a different period of times in SBF along with untreated glass base. The sample without SBF treatment (zero weeks) shows typical calcium-phosphate phases beside other phases as a result of the sintering process.

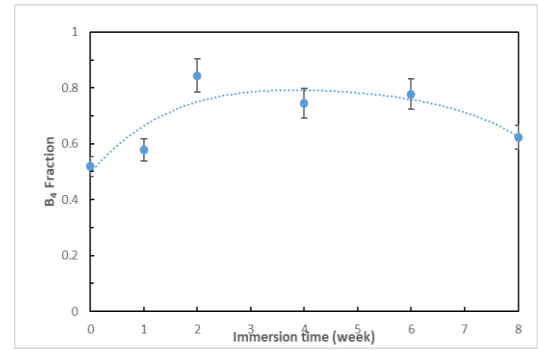


Figure 4. The concentration of B_4 fraction of the modified SG-PVP scaffold with the immersion time.

After exposing to SBF solution, it can be observed that for all various exposed period the XRD pattern match well with the standard one of HA (JCPDS No.: 72-1243). The changes in peaks intensity at each exposing period related to the nature of the corrosion mechanism of the modified glass as mentioned before and that confirmed the data obtained from the FT-IR analysis.

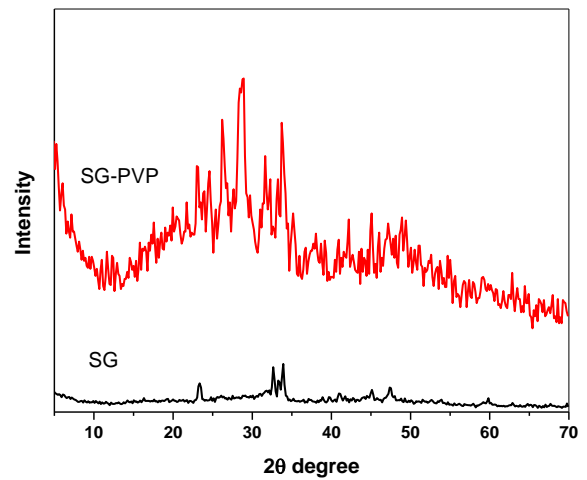


Figure 4. XRD spectra of the modified sintered glass SG and SG-PVP.

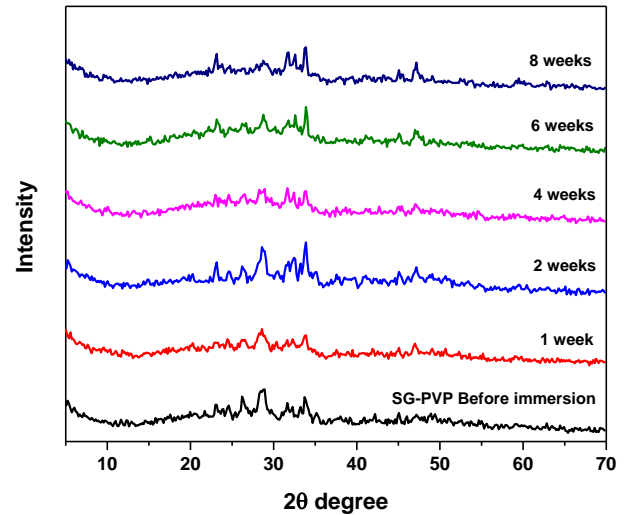


Figure 5. XRD spectra of the modified SG-PVP before and after exposing to SBF solution.

3.3. Scanning Electron Microscopic (SEM).

Figure 6, 7 illustrates the SEM-EDX images of the modified sintered glass SG-PVP surface morphology under static conditions before and after exposing to SBF solution for 4 weeks, and 8 weeks. The morphological features depicted that before exposing, the glass surface was nearly rough with small pores appeared on. After exposing for a short time, the surface

completely covered with a novel layer from fine flakes shaped species due to the interaction between the glass surface and the SBF solution. the morphology of the modified glass surface after 8 weeks of exposing to SBF solution changed significantly. The species aggregated together formed a dense apatite layer on the surface. The formation of apatite layer was confirmed before by the other analysis.

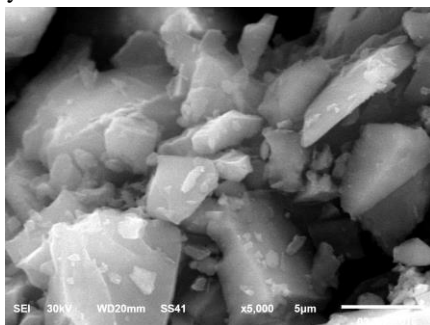


Figure 6. SEM image of the base sintered glass surface (SG).

The corresponding EDX spectrum of the prepared glass indicates that it is composed of K, Na, P, Ca, and O with the shown peak ratios. The peak belonging to B exists quite far from this detection limit and it is focused on the ratio of relative intensities of Ca:P peaks. EDX analysis before exposing to SBF showed a Ca/P atomic ratio equal to 5.50, a value which was close to that

calculated from the nominal composition of the starting glass. By increasing exposing time to SBF solution, the Ca/P ratio become 1.80 and 1.57 after 4 and 8 weeks, respectively. Stoichiometric hydroxyapatite has a Ca/P = 1.67.

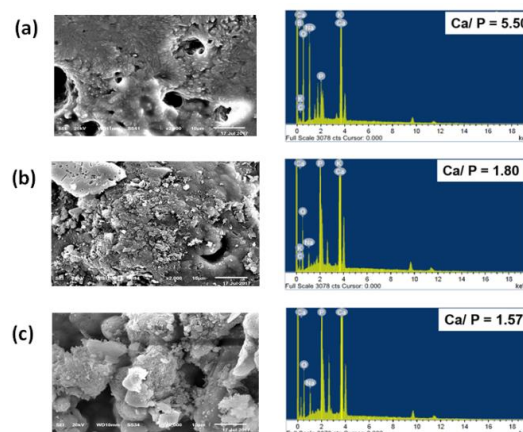


Figure 7. SEM- EDX images of the modified sintered glass surface (SG-PVP), before (a) and after exposing to SBF for four (b) and eight (c) weeks.

4. CONCLUSIONS

The bio glass containing (45% B₂O₃, 24.5% CaO, 24.5% Na₂O and 6% P₂O₅ all in mol. %) was elaborated by melting method. The “in vitro” assays were carried out by soaking of glass disks in SBF solution at different times. Evolution and growth of HA layer on glass surfaces have been followed using FT-IR , XRD, SEM and EDX. FT-IR absorption spectra and deconvolution the FT-IR spectra of all samples into their separated component bands confirm that the increasing of borate

glass bioactivity by increasing the period time of soaking until 6 weeks of soaking, then abruptly decreases. The X-ray diffraction confirmed the results from FT-IR and confirm the formation of a bioactive hydroxyapatite layer on the surface of bio glass after soaking in SBF solution. The SEM showed a visible and dense apatite layer after 8 weeks of immersion. These results represent an indicator of the potential bone bonding ability of the studied modified borate glass

5. REFERENCES

- Hench, L. Bioceramics. *J. Am. Ceram. Soc.* **1998**, *81*, 1705-1728, <https://doi.org/10.1111/j.1151-2916.1998.tb02540.x>.
- Hench, L. The story of bioglass®. *J Mater Sci: Mater Med* **2006**, *17*, 967-978, <https://doi.org/10.1007/s10856-006-0432-z>.
- Abdelghany, A.M.; El Batal, H.A.; Ramadan, R.M. Compatibility and bone bonding efficiency of gamma irradiated Hench's Bioglass-Ceramics. *Ceramics International* **2018**, *44*, 7034-7041, <https://doi.org/10.1016/j.ceramint.2018.01.138>.
- Hench, L.; Polak, J. Third-generation biomedical materials. *Science* **2002**, *295*, 1014-1017, <https://doi.org/10.1126/science.1067404>.
- El Batal, H.A.; El-Kheshen, A.A.; Ghoneim, N.A.; Marzouk, M.A.; El Batal, F.H.; Fayad, A.M.; Abdelghany A.M.; El-Beih, A.A. In Vitro Bioactivity Behavior of Some Borophosphate Glasses Containing Dopant of ZnO, CuO or SrO Together with their Glass-Ceramic Derivatives and their Antimicrobial Activity. *Silicon* **2019**, *11*, 197-208, <https://doi.org/10.1007/s12633-018-9845-9>.
- Singh, A. Hydroxyapatite, a biomaterial: Its chemical synthesis, characterization and study of biocompatibility prepared from shell of garden snail, *Helix aspersa*. *Bull. Mater. Sci.* **2012**, *35*, 1031-1038, <http://dx.doi.org/10.1007/s12034-012-0384-5>.
- Hench, L.; Wilson, J. Surface-active biomaterials, *Science* **1984**, *6*, 226-630, <https://doi.org/10.1126/science.6093253>.
- Ducheyne, P.; Qui, Q. Bioactive ceramics: The effect of surface reactivity on bone formation and bone cell function. *Biomaterials* **1999**, *20*, 2287-303, [https://doi.org/10.1016/S0142-9612\(99\)00181-7](https://doi.org/10.1016/S0142-9612(99)00181-7).
- Cerruti, M. Characterization of bioactive glasses. Effect of the immersion in solutions that stimulates body fluids., University of Turin Department of chemistry IFM Ph.D. thesis, Phd in chemical science 2001/2004.
- Shi, J.; Alves, N.; Mano J. Thermally Responsive Biomineralization on Biodegradable Substrates. *Adv. Funct. Mater.* **2007**, *17*, 3312-3318, <https://doi.org/10.1002/adfm.200601206>.
- Rahaman, M.; Day, D.; Bal, B.; Fu, Q.; Jung, S.; Bonewald, L.; Tomsia, A. Bioactive glass in tissue engineering. *Acta Biomater* **2011**, *7*, 2355-2373, <https://doi.org/10.1016/j.actbio.2011.03.016>
- Hench, L.; Splinter, R.; Allen, W.; Greenlee, T. Bonding mechanisms at the interface of ceramic prosthetic materials. *J. Biomed. Mater. Res.* **1971**, *5*, 117-141, <https://doi.org/10.1002/jbm.820050611>.
- Liu, X.; Pan, H.; Fu, H.; Fu, Q.; Rahaman, M.; Huang, W. Conversion of borate-based glass scaffold to hydroxyapatite in dilute phosphate solution. *Biomedical Materials* **2010**, *5*, 015-005, <https://doi.org/10.1088/1748-6041/5/1/015005>.

14. Huang, W.; Rahman, M.; Day, D.; Li, Y. Mechanisms for converting bioactive silicate, borate, and borosilicate glasses to hydroxyapatite in dilute phosphate solutions. *Physics and Chemistry of Glasses: European Journal of Glass Science and Technology Part B* **2006**, *47*, 647-658.
15. Hutmacher, D. Scaffolds in tissue engineering bone and cartilage. *Biomaterials* **2000**, *21*, 2529-2543, [https://doi.org/10.1016/S0142-9612\(00\)00121-6](https://doi.org/10.1016/S0142-9612(00)00121-6).
16. Liu, C.; Xia, Z.; Han, Z.; Hulley, P.; Triffitt, J.; Czernuszka, J. Novel 3D collagen scaffolds fabricated by indirect printing technique for tissue engineering. *J. Biomed. Mater. Res. B* **2008**, *58*, 519-528, <https://doi.org/10.1002/jbm.b.30975>.
17. Kokubo, T.; Kushitani, H.; Otsuki, C.; Sakka, S.; Kitsugi, T.; Yamamuro, T.J. Ion Release & Recharge, Wear, Gloss & Hydroxyapatite Formation. *Biomed. Mater. Res.* **1990**, *24*, 721.
18. Kokubo, T.; Takadama, H. Simulated body fluid and the novel bioactive materials derived from it. *Biomaterials* **2006**, *27*, 2907, <https://doi.org/10.1002/jbm.a.36620>.
19. Menazea, A.A.; Abdelghany, A.M.; Osman, W.H.; Hakeem, N.A.; El-Kader, F.A. Precipitation of silver nanoparticles in silicate glasses via Nd: YAG nanosecond laser and its characterization. *Journal of Non-Crystalline Solids* **2019**, *513*, 49-54, <https://doi.org/10.1016/j.jnoncrysol.2019.03.018>.
20. Reyna, A.; Hernandez, D.; Gorokhovskiy, A.; Robles, J.; Bocardo J.C. In vitro bioactivity assessment and mechanical properties of novel calcium titanate/borosilicate glass composites. *Ceram. Int.* **2011**, *37*, 1625, <https://doi.org/10.1016/j.ceramint.2011.01.034>.
21. El-Kader, F.A.; Hakeem, N.A.; Osman, W.H.; Menazea, A.A.; Abdelghany, A.M. Nanosecond laser irradiation as new route for silver nanoparticles precipitation in glassy matrix. *Silicon* **2019**, *11*, 377-381, <https://doi.org/10.1007/s12633-018-9890-4>.



© 2019 by the authors. This article is an open access article distributed under the terms and conditions of the Creative Commons Attribution (CC BY) license (<http://creativecommons.org/licenses/by/4.0/>).